

# Tunable lenses using transparent dielectric elastomer actuators

Samuel Shian,<sup>\*</sup> Roger M. Diebold, and David R. Clarke

School of Engineering and Applied Sciences, Harvard University, Cambridge, Massachusetts 02138, USA

<sup>\*</sup>[sshian@seas.harvard.edu](mailto:sshian@seas.harvard.edu)

**Abstract:** Focus tunable, adaptive lenses provide several advantages over traditional lens assemblies in terms of compactness, cost, efficiency, and flexibility. To further improve the simplicity and compact nature of adaptive lenses, we present an elastomer-liquid lens system which makes use of an inline, transparent electroactive polymer actuator. The lens requires only a minimal number of components: a frame, a passive membrane, a dielectric elastomer actuator membrane, and a clear liquid. The focal length variation was recorded to be greater than 100% with this system, responding in less than one second. Through the analysis of membrane deformation within geometrical constraints, it is shown that by selecting appropriate lens dimensions, even larger focusing dynamic ranges can be achieved.

©2013 Optical Society of America

**OCIS codes:** (010.1080) Active or adaptive optics; (220.3620) Lens system design; (160.5470) Polymers; (230.2090) Electro-optical devices.

---

## References and links

1. H. Ren and S.-T. Wu, *Introduction to adaptive lenses* (Hoboken, New Jersey: John Wiley & Sons, Inc., 2012).
2. M. Blum, M. Büeler, C. Grätzel, and M. Aschwanden, "Compact optical design solutions using focus tunable lenses," in *SPIE Proc.* **8167**, (2011).
3. G. C. Knollman, J. L. S. Bellin, and J. L. Weaver, "Variable-focus liquid-filled hydroacoustic lens," *J. Acoust. Soc. Am.* **49**(1B), 253–261 (1971).
4. N. Sugiura and S. Morita, "Variable-focus liquid-filled optical lens," *Appl. Opt.* **32**(22), 4181–4186 (1993).
5. H. Ren and S.-T. Wu, "Variable-focus liquid lens," *Opt. Express* **15**(10), 5931–5936 (2007).
6. F. Schneider, J. Draheim, C. Müller, and U. Wallrabe, "Optimization of an adaptive PDMS-membrane lens with an integrated actuator," *Sensor Actuat. A.* **154**(2), 316–321 (2009).
7. H.-M. Son, M. Y. Kim, and Y.-J. Lee, "Tunable-focus liquid lens system controlled by antagonistic winding-type SMA actuator," *Opt. Express* **17**(16), 14339–14350 (2009).
8. G. Beadie, M. L. Sandrock, M. J. Wiggins, R. S. Lepkowitz, J. S. Shirk, M. Ponting, Y. Yang, T. Kazmierczak, A. Hiltner, and E. Baer, "Tunable polymer lens," *Opt. Express* **16**(16), 11847–11857 (2008).
9. F. Carpi, G. Frediani, S. Turco, and D. De Rossi, "Bioinspired tunable lens with muscle-like electroactive elastomers," *Adv. Funct. Mater.* **21**(21), 4152–4158 (2011).
10. S. Shian, R. M. Diebold, A. McNamara, and D. R. Clarke, "Highly compliant transparent electrodes," *Appl. Phys. Lett.* **101**(6), 061101 (2012).
11. S. I. Son, D. Pugal, T. Hwang, H. R. Choi, J. C. Koo, Y. Lee, K. Kim, and J.-D. Nam, "Electromechanically driven variable-focus lens based on transparent dielectric elastomer," *Appl. Opt.* **51**(15), 2987–2996 (2012).
12. H. Wang, S. Cai, F. Carpi, and Z. Suo, "Computational model of hydrostatically coupled dielectric elastomer actuators," *J. Appl. Mech.* **79**(3), 031008 (2012).
13. P. Brochu and Q. Pei, "Advances in dielectric elastomers for actuators and artificial muscles," *Macromol. Rapid Commun.* **31**(1), 10–36 (2010).
14. R. Pelrine, R. Kornbluh, Q. Pei, and J. Joseph, "High-speed electrically actuated elastomers with strain greater than 100%," *Science* **287**(5454), 836–839 (2000).
15. F. Carpi, G. Frediani, M. Nanni, and D. De Rossi, "Granularly coupled dielectric elastomer actuators," *IEEE/ASME Trans. Mechatronics* **16**(1), 16–23 (2011).

---

## 1. Introduction

Compact, adaptive focus lenses are attractive for imaging applications where space is at a premium, including endoscopes, cell phone cameras, and machine vision apparatus. By

varying either the refractive index of the optical medium or the lens curvature, adaptive lenses can supplant the bulky and expensive gears and electrical motor assemblies found in traditional focus tunable lenses [1,2]. Refractive index variation is typically limited to specific liquid crystal materials which have inherent optical limitations, such as polarization effects and relatively slow response times [2]. Lens curvature variation makes use of either electrowetting principles to alter the position of two immiscible liquids of different refractive index or deform flexible membranes encapsulating a liquid [1]. Within this second category of flexible membrane lenses, the lens shape is altered in one of two ways: internal volume change through liquid mass transfer [3,4] or lens periphery actuation to induce deformation in the optical path, either in the thickness or radial direction [2], [5–9]. A variety of actuation mechanisms are used to drive the deformation of these tunable lenses, including electric motors, rotating screws, piezoelectric elements, or dielectric elastomer actuators (DEAs). However, each of these existing adaptive lens configurations locates the actuator outside the optical path. The consequence of placing the actuator outside the optical path is that a significant fraction of the lens' lateral area is occupied by the actuating mechanism, reducing the usable optical area [2].

The recent demonstration of compliant, highly transparent, and electrically conductive electrodes in combination with dielectric elastomers affords the opportunity to use an electrical signal to alter the shape of a liquid lens without external actuation [10]. The high optical transparency of the electrodes, liquid, and elastomer permits the construction of simple, self-contained adaptive lenses suitable for space-constrained tasks. The use of transparent DEAs for lenses was recently demonstrated, but as the lens consists of a buckling solid elastomer membrane, it only operates as a diverging optic [11]. The purpose of this communication is to describe a self-contained tunable lens with an integrated electrical actuator in the optical path of the lens. A detailed description of the design, materials, and fabrication of the lens are presented in the following sections. Additionally, an analysis of the membrane deformation and optical properties of the lens will be discussed.

## 2. Lens design

The lens is constructed from a stiff frame, a transparent liquid of fixed volume, and two elastomeric membranes, one passive and the other electroactive, as shown in Fig. 1. The electroactive membrane is a transparent dielectric elastomer coated with transparent compliant electrodes on both sides; in this case, the dielectric elastomer is a commercially available acrylic elastomer and the electrodes are single walled carbon nanotube (SWCNT) mats. The focal length and the numerical aperture of the lens in the rest state are determined by both the refractive index of the liquid and the extent of the membrane bulging. The latter is controlled by the volume of the liquid placed in inside the cavity; more liquid reduces the focal length and increases the numerical aperture of the lens. The focal length of the lens can be designed to increase or decrease upon actuation depending on the location of the electroactive membrane, i.e., as the larger or smaller diameter membrane, respectively. Consequently, if both membranes are electroactive, the focal length of the lens can increase or decrease relative to the rest state, depending on which membrane is actuated. However, the transparency of the lens with two electroactive membranes will suffer from the presence of an additional electrode pair. Since the diameter of each membrane is constant, the actuation will also change the numerical aperture of the lens, which is inversely proportional to the focal length.

The lens' adaptive capability is driven by the relative difference in curvature of each membrane as a function of the internal liquid pressure. This capability is accomplished by making the diameters of the membrane windows,  $D_1$  and  $D_2$ , unequal, allowing the curvature change to be different in the two membranes. As shown below, the percent change in focal length as well as the absolute focal range depends on the geometrical configuration of the assembly, the liquid volume, and the mechanical properties of the elastomer membranes. The

internal liquid pressure is controlled by the actuation of the DEA membrane. When a voltage is applied to the DEA, the Coulombic attraction between the charges generates a Maxwell stress over the membrane's thickness and subsequently displaces volume in the plane of the electrodes. As the DEA deforms, the tension in the membrane decreases causing a concomitant decrease in liquid pressure, altering the DEA and passive membrane curvature and thus the focal length of the lens.

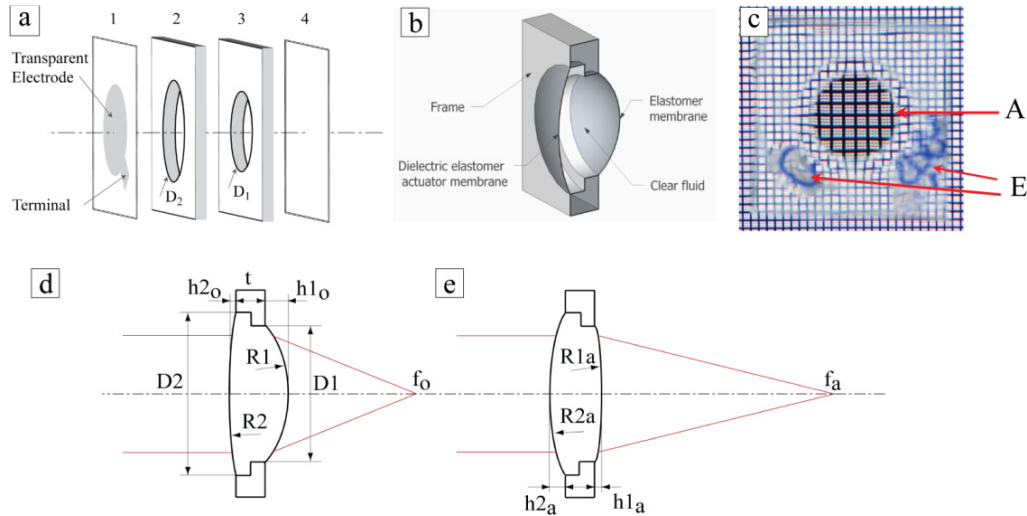


Fig. 1. (a) Construction of the tunable lens, consisting of 3 main parts: dielectric elastomer actuator membrane (part 1), frame (parts 2 and 3), and passive elastomer membrane (part 4). The aperture of the lens is defined by the smallest diameter of the frame cavity or  $D_1$ . (b) 3-D cross-section of a fully assembled lens. (c) Optical photograph of the tunable lens as viewed along the optical axis and against a black background grid (1 mm grid spacing). The lens aperture (A) and transparent electrode terminals (E) are shown; electrode terminals are identified by blue circles drawn in marker on the device. (d) Schematic of the lens at the rest state (subscripted as 'o') and (e) during actuation (subscripted as 'a'), showing a change in focal length.  $D$ ,  $h$ , and  $R$  are the diameter, height, membrane curvature, respectively. Suffix 1 and 2 refer to the passive and the electroactive membranes, respectively. The frame thickness,  $t$ , and the lens focal length,  $f$ , are also depicted.

To analyze the lens design's focal tunability, a MATLAB script was written to calculate the maximum focal length change at the maximum actuation as a function of  $D_2/D_1$  and initial membrane height,  $h_{1o}/D_1$  (see Fig. 1(d), 1(e)). This calculation has several assumptions. Spherical approximation is assumed, permitting use of the thick lens equation. As shown later, the spherical approximation requires that bulging be relatively small ( $h_1/D_1 < 0.15$ ,  $h_2/D_2 < 0.15$ ). Additionally, the initial height,  $h_{2o}$ , is arbitrarily defined as 2.5% of  $D_2$ . Consequently, when  $D_2$  is larger than  $D_1$ , membrane 2 is chosen to be stiffer than membrane 1 in order to ensure high curvature of  $D_1$  relative to  $D_2$  at rest. In practice, the membrane stiffness can be achieved by choosing a combination of various pre-stretch, thickness, or material (elastic constant) values. Gravitational effects are neglected and positive pressure, thus convex membrane shapes, is assumed.

The resulting calculation is shown in Fig. 2. When  $D_2$  and  $D_1$  are equal, the increase in one membrane's curvature during constant volume actuation is compensated by a reduction in curvature of the other membrane, resulting in zero focal length change, shown by the white area at  $D_2/D_1 \sim 1$ . In general, increasing the initial membrane height,  $h_{1o}/D_1$ , and increasing the refractive index of the liquid decreases the initial focal length. However, the refractive index does not affect the relative focal length change.

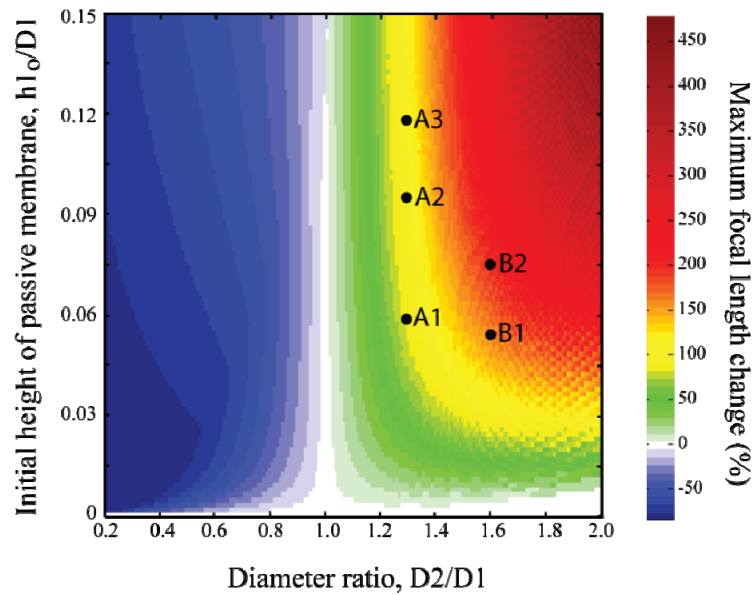


Fig. 2. Calculated maximum focal length change (color coded) with respect to the initial focal length, as a function of the membrane diameter ratio,  $D2/D1$ , and initial membrane 1 height,  $h1_o/D1$ . Black dots represent lens prototypes whose actuation is characterized in Fig. 4.

Figure 2 can be divided into two regions. In the first, where  $D2/D1 < 1$ , the focal length change is negative, indicating that the focal length decreases with actuation. In the second region, where  $D2/D1 > 1$ , the focal length change is positive, indicating that the focal length increases with actuation. In this second region, above 10% initial height  $h1_o/D1$ , the maximum focal length change increases with increasing membrane diameter difference. However, at relatively low initial  $h1_o/D1$  values ( $< 0.01$ ), higher  $D2/D1$  does not increase the maximum focal length change. This is mainly attributable to the limited actuation achievable while maintaining positive liquid pressure. The large actuation strain of the dielectric elastomer can only be utilized fully at high initial  $h1_o/D1$  values, where enough cap volume is available for displacement through actuation.

In Fig. 2, the maximum focal length change in the first region occurs at the opposite corner from that of the second region, i.e., upper right and lower left corners, respectively. To optimize the lens geometry for maximum focal length change, the active and passive membranes should initially possess low and high curvature, respectively, as the DEA membrane can only increase in curvature. Therefore, in order to maximize the focal length change when  $D2/D1 > 1$ , the passive membrane,  $D1$ , is at high curvature in the rest state, which corresponds to the upper right corner of Fig. 2. Alternatively, when  $D2/D1 < 1$ , the configuration for maximum focal length change corresponds to the lower left corner of Fig. 2.

### 3. Fabrication

A pair of lens frames was prepared from a cast polydimethylsiloxane (PDMS) sheet (Sylgard 184, Dow Corning) cut into a rectangular solid (25 mm x 25 mm x 2 mm). To define the active diameter of the lens membranes, one frame was punched in the center with diameter  $D1$  and the other with diameter  $D2$ . The passive elastomer membrane was made from 0.5 mm thick acrylic elastomer (VHB 4905, 3M) biaxially pre-stretched with a linear strain of 100%, while the electroactive elastomer membrane was made from 1 mm thick acrylic elastomer (VHB 4910, 3M) biaxially pre-stretched with a linear strain of 300%. According to the manufacturer's datasheet, both membranes have a refractive index of 1.476. SWCNT electrodes were deposited on both sides of the electroactive membrane using the filtration-

transfer method described previously [10]. These components were then bonded using silicone adhesive (Silpoxy, Reynolds Manufacturing), as shown in Fig. 1(a). After curing, clear silicone oil (Dow Corning Liquid 200, 50cSt, refractive index 1.4022) was injected into the lens cavity. Connections to the electrodes were made using wires punched through the PDMS frame. One lens prototype is depicted in Fig. 1(c) against a square grid background, illustrating that all materials, including the frame, are optically transparent; the frames can be made opaque to prevent stray light if preferred. The curvature of the lens is evident in the magnified image of the background square pattern. The lens focal length was measured with the same setup shown in Fig. 3(b), using the most distant object possible, located more than 75x the longest focal length measured. Using a linear servo, the lens is translated along its optical axis until the sharpest image on the sensor plane is obtained, determined by an edge detection algorithm using LabVIEW software. The focal length is approximated by the distance from the image sensor plane to the lens frame surface facing the sensor. The procedure is repeated for various lens actuation states.

#### 4. Results

In principle, the presented lens concept can be applied from sub-millimeter to centimeter lens diameters depending on the membrane thickness and density of the liquid. However, for ease of fabrication, we chose dimensions shown in Fig. 1(c) using commercially available materials. Although the DEA membrane is made from an acrylic material and is not optimized for optical transparency, it contributes only a small amount of absorption. Additionally, the reflective light loss by the membrane surface can be significant in the absence of anti-reflective coatings. The assembled lens has typical optical transmittance of 88% at 550 nm.

To qualitatively assess the optical performance of the lens, images of objects located at different distances were projected through the lens onto a complementary metal oxide semiconductor (CMOS) camera sensor. During testing, the lens was mounted at a fixed distance from the camera and the actuation voltage was adjusted until the sharpest image of each object was displayed, indicative of the focal plane. The experimental setup and captured images are shown in Fig. 3. The lens can be seen to produce relatively sharp images of the objects, showing minimal chromatic and astigmatism aberrations. The blurring of out-of-focus objects in each frame illustrates a small depth of field, indicative of a relatively large numerical aperture. The device numerical apertures are estimated to be 0.2 to 0.25 over the entire imaging range, which are comparable to commercially available tunable lenses [2]. Higher numerical apertures can be achieved by decreasing the initial focal length.

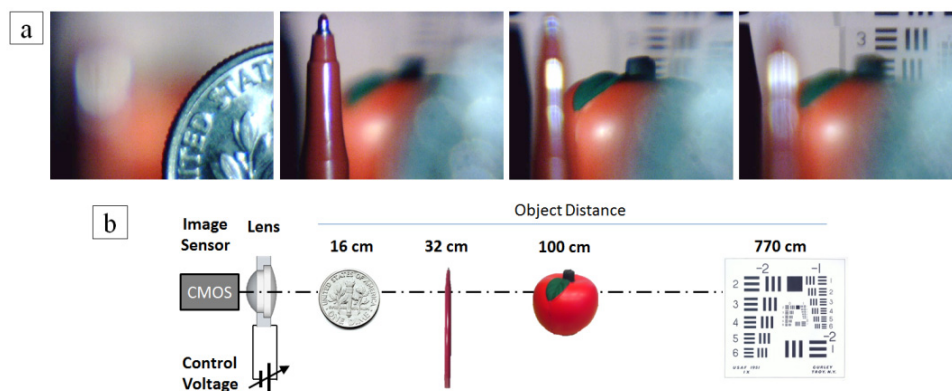


Fig. 3. (a) Photographic images at various focal lengths as captured by a CMOS image sensor demonstrating the focusing capability of the lens. (b) A schematic of the measurement setup used for image acquisition.

As the tunable lens changes shape, the membranes experience deformation, whose magnitude generally depends on the curvature. The passive membrane, D1, is subjected to hydrostatic pressure which exerts a uniform normal force. Because the membrane is constrained at the edge, however, the local membrane deformation varies radially, reaching a maximum at the membrane center. During actuation, the DEA membrane, D2, is under combined hydrostatic pressure and Maxwell stress,  $\sigma_M$ , defined as

$$\sigma_M = \epsilon \left( \frac{V}{t} \right)^2, \quad (1)$$

where  $\epsilon$ ,  $V$ , and  $t$  are the dielectric permittivity, electrical potential, and elastomer thickness, respectively. Since the membrane thickness varies along the radial distance, the local Maxwell stress is inversely proportional to the square of the local thickness, resulting in a non-uniform actuation strain generated radially when a constant voltage is applied.

To assess how the non-uniform Maxwell stress affects the optical properties of the lens, the membrane curvature under various electrical fields needs to be analyzed. Wang et al. developed an analytical model for hydrostatically coupled dielectric elastomer actuators [12] similar to the present tunable lens configuration. In the model, the Maxwell stress is coupled with the mechanical deformation of the elastomer membranes through a neo-Hookean hyper-elastic material model. The analytical model was solved numerically and the resulting deformation profiles of the dielectric elastomer membrane under various electrical fields were compared to spherical profiles. We find that at relatively low membrane curvature,  $h/D < 0.15$ , the spherical cap geometry approximates the membrane shape well; the validity of the spherical cap geometry is verified from the measurement of the lens profile. However, at relatively high deformations,  $h/D > 0.15$ , the membrane shape becomes increasingly parabolic, causing the center portion of the membrane to strain significantly more relative to the area near the perimeter. In practice, the optically active area of the lens can be limited to the area near the optical axis using a circular aperture, such that spherical curvature is maintained within the smaller aperture and thus image distortion can be minimized at high membrane deformation.

For a given lens dimensions D1 and D2, the initial focal length,  $f_o$ , is determined by the volume and refractive index,  $n$ , of the liquid. As the volume of liquid is increased, the lens membranes bulge more, decreasing the  $f_o$ . Using the aforementioned spherical curvature approximation, the focal length of the lens can be calculated using the thick lens equation

$$\frac{1}{f} = (n-1) \left[ \frac{1}{R_1} - \frac{1}{R_2} + \frac{(n-1)d}{nR_1R_2} \right]. \quad (2)$$

We found that the calculated focal length agrees well with the observed focal length. For example, the calculated and observed focal lengths for one of the fabricated lenses are 28.4 mm and  $29 \pm 1$  mm, respectively. During actuation, the electroactive membrane stretches, decreasing R2 while increasing R1. The resulting net curvature change and the corresponding change in the focal length originates from the relative difference in the diameter D2 with respect to D1. As shown in Fig. 2, the relative difference D2/D1 plays an important role in the amount of focal length change.

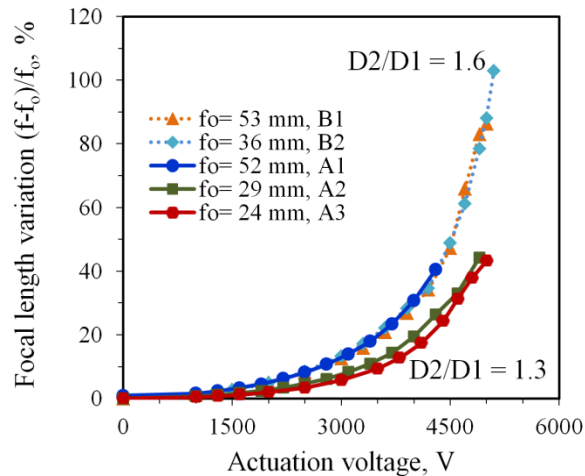


Fig. 4. Focal length variation as function of actuation voltage and initial focal length,  $f_0$ . A and B refer to the fabricated lenses with dimensions shown in Fig. 2.

Figure 4 depicts the change in lens focal length with actuation voltage for several geometrical configurations, and illustrates that the maximum achievable focal length is influenced by the membrane diameter ratio,  $D2/D1$ . At actuation voltages greater than 4900 V, the recorded images are degraded significantly due to non-concentric lens deformation, thus defining the maximum usable actuation voltage. The liquid pressure inside the lens drops monotonically with actuation strain [12], and at a critical strain, the holding pressure of the membrane is overcome by gravitational forces acting on the liquid. Since the optical axis in our lens is perpendicular to the gravitational force vector, the membrane curvature deforms asymmetrically and distorts the image [4]. Such deformation is minimized if the lens optical axis is parallel to the gravitational force, allowing for higher actuation strain and thus larger focal length change than that of the perpendicular configuration.

The trend of focal length changes in lenses A and B agree with the calculated values in Fig. 2. Fabricated lenses A1, A2, and A3 have different initial passive membrane heights, but due to identical  $D2/D1$  values, they have similar maximum focal length change values as predicted by the calculation. Large  $D2/D1$  values can be seen to increase the maximum possible focal length change, as shown by comparing the maximum focal length change of lenses B vs. A in Fig. 4, i.e., ~100% vs. ~45%. In the calculation, the final  $h1/D1$  essentially becomes zero at the maximum focal length change as the passive membrane becomes flush with the frame. In practice, due to aforementioned gravitational effects, the pressure drop within the lens at maximum actuation may deform membrane D2 non-concentrically, causing image distortion. This gravity induced distortion is pronounced when the optical axis is perpendicular to the gravitational vector, decreasing the effective maximum focal length change. Such effects are observed in the fabricated lenses, where the measured maximum focal length change is approximately half of the calculated value. For example, the observed and the calculated maximum focal length change are 103% and 200%, respectively for lens B2. Nevertheless, such a discrepancy is not as large as it may seem since the focal length change is non-linear, i.e., the actuated focal length can be very large or approach infinity within a small membrane height change. Although not directly addressed in this work, the lens could theoretically be made small enough such that viscous and interfacial effects will dominate over gravitational effects, ameliorating the non-concentric bulge concern.

The response time of the lens is determined by the amount of strain (i.e., the amount of displaced liquid mass) and the DEA actuation power. The actuation power is proportional to the rate of electrical charge delivered to the electrodes and the total electrical energy stored within the DEA volume. While DEAs can exhibit relatively fast response times in comparison



to other electroactive polymer actuators [13,14], the liquid's inertia slows the response time of the lens system; the more liquid being moved, the longer the response time. Our lenses have response times of the order of tens to hundreds of milliseconds. Similar DEA configurations reported in literature by Carpi et al. indicate that a relatively high frequency response, in excess of one hundred hertz, is possible but at limited actuation strains [15]. Appropriate lens parameters, such as reduced lens dimensions, the use of low density and low viscosity liquids, and elastomer membranes with high stiffness can be applied to further optimize the system for improved actuation speed. Furthermore, improved dielectric elastomer materials, with increased dielectric permittivity and reduced viscous losses, can decrease the driving voltage for actuation and increase actuation speed, respectively.

## **7. Conclusions**

Electrically tunable adaptive lenses have been demonstrated with a transparent actuator located directly in the optical path. Lenses built using this concept yield focal length changes of more than 100% at relatively fast response times ( $< 1$  s). The lens performance is consistent with the mechanics of elastomer deformation and relatively large focal length changes, of hundreds of percent, can be achieved by choosing an appropriate lens geometry.

## **Acknowledgments**

The authors acknowledge the partial financial support by the Harvard MRSEC program of the National Science Foundation under Award number DMR-0820484.